Heliyon 6 (2020) e05080

Contents lists available at ScienceDirect

Heliyon

journal homepage: www.cell.com/heliyon

Research article

Catalytic assessment of solid materials for the pyrolytic conversion of low-density polyethylene into fuels

Melisa Olivera [a], Mauricio Musso [a], Andrea De León [a], Elisa Volonterio [b], Alejandro Amaya [a,c], Nestor Tancredi [a,c], Juan Bussi [a,*]

[a] Laboratorio de Fisicoquímica de Superficies, DETEMA, Facultad de Química, Udelar, Gral. Flores 2124, 11800, Montevideo, Uruguay
[b] Área Grasas y Aceites, Departamento de Ciencias y Tecnología de Alimentos, Facultad de Química, Udelar, Gral. Flores 2124, 11800, Montevideo, Uruguay
[c] Instituto Polo Tecnológico de Pando, Facultad de Química, Udelar, By pass Ruta 8 y Ruta 101 s/n, Pando, Canelones, Uruguay

ARTICLE INFO

Keywords:
Chemical engineering
Energy
Environmental science
Industrial chemistry
Materials science
Polyethylene recycling
Fuels production
Pyrolysis
Catalysts

ABSTRACT

Pyrolysis techniques provide an interesting way of recycling plastic wastes (PW) by transforming them into liquid fuels with high calorific values. Catalysts are employed in PW pyrolysis in order to favor cracking reactions; in that regard, cheap and abundant natural resources are being investigated as potential catalyst precursors. This article explores the pyrolysis of low-density polyethylene (LDPE) in a semibatch reactor under a reduced pressure of 300 torr and temperatures in the range of 370 °C–430 °C. Three different solid materials, an activated carbon (AC1), a commercial Fluid cracking catalyst (FCC) and an aluminum- pillared clay (Al-PILC), were tested as catalysts for the pyrolysis process. Thermogravimetric analyzes were previously performed to select the most catalytically active materials. AC1 displayed very low catalytic activity while FCC and Al-PILC displayed high activity and conversion to liquid products. Hydrocarbons ranging from C5 to C28 were identified in the liquid products as well as significant changes in their composition when FCC and Al-PILC catalyst were used. Differences in the catalytic activity of the 3 solid materials are ascribed mainly to differences in their acid properties.

1. Introduction

Plastics have become an essential part of our society because of their versatile applications that formerly relied on other traditional materials such as metal, glass, wood and natural fibers (mainly cotton and wool). For most applications, stability and durability have been improved, and hence they are considered synonymous with materials that are resistant to many environmental constraints. However, there is a growing concern about the harmful effects of plastic waste (PW) due to its accumulation and consequent pollution of terrestrial and aquatic ecosystems. Several technical approaches involving physical and chemical processes have been developed to perform PW recycling. Among them, those involving thermochemical treatmeants, namely pyrolysis techniques, have gained attention as they provide an opportunity of transforming plastics into high-energy-density fuels, with high calorific values that match conventional fuels (e.g. gasoline, kerosene, diesel, etc.) [1, 2, 3, 4, 5, 6]. In a typical pyrolysis process, long chain organic polymers are converted into smaller and less complex ones with the use of heat (450–800 °C) [6, 7, 8]. Gases, oils and chars are obtained in different proportions depending on the operating conditions. The hydrocarbon mixture obtained, could be further processed either in petrochemical refineries or in standalone recycling processes [7, 8].

Catalysts are employed in PW pyrolysis to favor cracking reactions, thus allowing the use of lower temperatures and reducing the process energy demand [9, 10, 11, 12, 13, 14]. Catalysts also help to improve fuels yield in the gasoline to diesel range, thus eliminating the necessity of further processing [15, 16]. The most common type of catalysts are heterogeneous and, among them, those based in zeolitic materials have been extensively researched. The acidity of their active sites and their crystalline microporous structure (textural properties) favor hydrogen transfer reactions involved in the cracking mechanism and thereby make them suitable for obtaining high conversions at relatively low temperatures, between 350 and 500 °C [15, 16, 17, 18, 19, 20, 21, 22]. Other non-zeolitic catalytic materials are reported, such as metal oxides, sulfated metal oxides, molecular sieves, Fluid cracking catalysts (FCC), metal carbonates and mesoporous materials [10, 12, 23, 24, 25].

In search of inexpensive new catalysts for PW pyrolysis, cheap and abundant natural resources are also being investigated as potential

* Corresponding author.
E-mail address: jbussi@fq.edu.uy (J. Bussi).

https://doi.org/10.1016/j.heliyon.2020.e05080
Received 26 June 2020; Received in revised form 6 September 2020; Accepted 23 September 2020

catalyst precursors. In this sense, activated carbons prepared from different carbonaceous source materials were reported to catalyze plastic pyrolysis allowing to obtain yields of liquid products greater than 95% at a reaction temperature of 240 °C and a vacuum pressure of about 300 mmHg [14]. Clay-based materials have also been reported as catalysts for plastics pyrolysis. Two natural clays were found to completely decompose polyethylene at a maximum temperature of 400 °C, with yields to liquid products of 70%, compared to less than 50% over US-Y zeolite [26]. The same authors also reported high selectivity and yield to liquid hydrocarbons using an Al-pillared saponite in the pyrolysis of polyethylene. The regenerated pillared clay, after combustion of the formed coke, showed practically the same behavior of its fresh counterpart regarding conversion and yield, as well as product distribution [27]. Other authors also found the superior efficiency of a Fe-pillared clay in relation to those pillared with Ti, Zr and Al working at 500 °C in a laboratory scale installation [28]. More recently, a calcium bentonite was found to significantly affect the rate of plastic pyrolysis at 500 °C. The yield of liquid products attained values in the range of 81–89% with the different types of plastics that were tested [29]. The use of a pelletized bentonite clay in a large-scale study allowed the obtention of pyrolysis oils with performance comparable to diesel in engine power tests [30].

Differences in the experimental conditions and reactors used in all the studies referred above do not allow to make suitable comparisons among catalysts, thus preventing a better knowledge about their relative efficiencies. Aiming to clarify this aspect, a preliminary study using a thermogravimetric technique was performed to have a first approach about the catalytic activity of different solid materials prepared from natural resources in the pyrolytic conversion of low-density polyethylene (LDPE) into volatile products. These materials include a series of activated carbons prepared from wood sawdust by a chemical method using H_3PO_4 which is among the most widely chemical reagents used to obtain a well-developed pore structure and increase the total specific surface area [31]. In addition, various acidic functional groups containing phosphorous can be created on the carbon surface and therefore improve its catalytic activity in the pyrolysis process [32]. Al and Fe pillared clays prepared from a clay mineral are also included in these studies. Pyrolysis of LDPE was accordingly performed with several of these solid materials. Comparison with a commercial activated carbon, a cracking catalyst and some other materials is also included.

2. Experimental methods

2.1. Catalysts synthesis

Eucalyptus Dunnii (ED) with a moisture content of 8.7% served as the precursor to produce activated carbons. ED sawdust was ground until a final size below 1 mm. Further, it was imbibed in a 20% (v/v) H_3PO_4 aqueous solution. The solution to wood relationship was fixed to obtain an $X_p = 1.9$, with X_p being the phosphorus to wood mass ratio. This X_p value was chosen to obtain a porous development that includes not only micropores but also mesopores, for obtaining good accessibility of molecules in liquid phase. The impregnation took place for 1 h at room temperature and 24 h at 95 °C. Activation was performed at 350 °C during 1 h in a tubular furnace under N_2 flow using a heating rate of 15 °C min^{-1}. A second activation at 450 °C was done using the same conditions. Activated carbons AC2 and AC3 were prepared in analogous conditions, with an H_3PO_4 aqueous solution of 28% (v/v), an $X_p = 1$, an impregnation temperature of 85 °C, a heating rate of 5 °C min^{-1} and an activation temperature of 400 °C and 350 °C for AC2 and AC3, respectively [31]. An aluminum oxide-pillared clay (Al-PILC) was prepared from a calcium-rich montmorillonite from Bañado de Medina, Uruguay, as reported elsewhere [33]. An iron oxide-pillared clay (Fe-PILC) was also prepared with the same clay as reported elsewhere [34, 35]. Other materials that were also tested are an activated carbon DARCO, the calcium-rich montmorillonite previously referred (Mont) and a commercial Fluid cracking catalyst (FCC) from Fábrica Carioca de Catalizadores, Brazil, all of them without any previous treatment.

2.2. Pyrolysis tests

They were performed in a semibatch reactor consisting of a 1-liter borosilicate reaction balloon connected to a condenser, which in turn is connected to a receiving balloon cooled with a water-ice bath (0 °C) (Figure 1). The whole system is connected to a vacuum pump in order to fix the operating pressure below 1 bar, which according to the literature allows the increase of the average molecular weight of the volatile products entering to the condenser and, therefore, the amount of condensate that gives rise to the liquid product [1, 12, 36]. The reaction balloon is placed into a heating mantle connected to a programmable temperature controller. In a typical run, LDPE film was previously cut into pieces of about 1 cm × 1 cm. 15 g of the pre-processed plastic was then charged into the reaction balloon together with 5 g of catalyst. This LDPE/catalyst ratio was selected according to several preliminary tests and also taking into account what several authors report about the experimental conditions leading to the highest yields of liquid product [27, 29, 37, 38]. The balloon was then attached to the condenser with a connecting elbow, the pressure was fixed in 300 torr and the temperature of the heating mantle was raised at a rate of 8 °C min^{-1} until 30 °C below the final reaction temperature. The final reaction temperature was attained with a heating ramp of 1 °C min^{-1}. The reaction was monitored by periodically measuring the volume of liquid product per unit of time at the condenser outlet, and by recording the temperature in the reaction balloon and in the elbow that connects the reactor balloon with the condenser. The mass of liquid collected in the receiving balloon and that of the solid residue in the reaction balloon were measured after the end of each test. The liquid yield was calculated according to Eq. (1):

$$Liquid\ yield = \frac{final\ mass\ of\ liquid\ in\ the\ receiving\ balloon * 100}{initial\ mass\ of\ LDPE} \quad (1)$$

2.3. Characterizations

(i) Thermogravimetric analysis (TGA). LDPE was melted and mechanically mixed with the catalyst in a proportion plastic/catalyst of 3:1 (w:w) which is similar to that which was subsequently used in the pyrolysis tests. After cooling, a sample of the solidified dispersion was analyzed in a Shimadzu TGA-50 equipment, from room temperature to 700 °C at a heating rate of 10 °C min^{-1}, under 50 ml min^{-1} of N_2 flow.

(ii) N_2 adsorption-desorption isotherms. They were executed for Al-PILC, FCC and AC1 catalysts at 77 K with a Beckman-Coulter SA 3100 equipment. The specific surface area was obtained by fitting results to the Brunauer, Emmett and Teller model (BET area), the

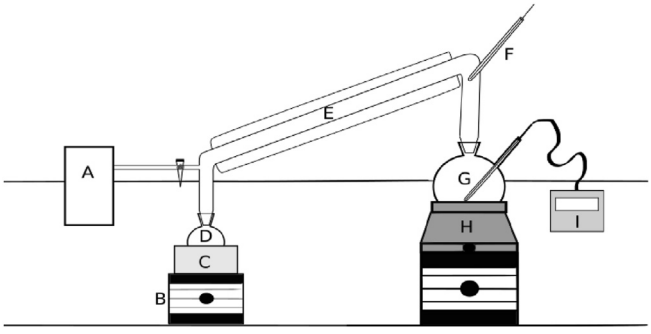

Figure 1. Reaction system diagram, where: A, vacuum pump with automatic control; B, holder; C, ice-water bath; D, collection balloon; E, condenser; F, thermocouple; G, reaction balloon; H, heating mantle and I, temperature controller.

micropore volume was calculated by fitting experimental values to the Dubinin-Radushkevich equation (VDR), and by isotherm extrapolation at Pr = 0,99 the total pore volume (V_T) was obtained.

(iii) Temperature-programmed desorption of NH_3 (TPD-NH_3). It was performed to characterize the acidity of Al-PILC, FCC and AC1 catalysts. The samples (200 mg) were treated in He (60 cm^3 min^{-1}) at 500 °C for 2 h and then exposed to a 1% NH_3/He stream for 40 min at 100 °C. Weakly adsorbed NH_3 was removed by flowing He at 100 °C for 2 h. The temperature was then increased at 10 K min^{-1} and the NH_3 concentration in the effluent was measured by mass spectrometry in a Baltzers Omnistar unit.

(iv) FTIR spectra. They were recorded to identify typical surface functional groups of Al-PILC, FCC and AC1 catalysts using a Bomem Hartmann & Braun MB-Series FTIR spectrometer as well as those in liquid products of the pyrolysis tests. Pellets were prepared by thoroughly mixing carbon and KBr at the 1:400 carbon/KBr weight ratio in a small size agate mortar. The resulting mixture was compacted in a Perkin-Elmer manual hydraulic press at 10 ton for 3 min.

(v) Heating value. The higher heating value (HHV) was determined for liquid products obtained in the pyrolysis tests using an oxygen bomb calorimeter Parr, model N° 1341.

(vi) Elemental analysis. It was performed for liquid products obtained in the pyrolysis tests using an Elemental Analyzer Thermo Flash 2000.

(vii) Chromatographic measurements. The liquid products of the pyrolysis were analyzed by gaseous chromatography under the following conditions: i) a Shimadzu GC2010 equipment, with on-column injection, a capillary column OPTIMA-1TG and a FID detector; ii) Shimadzu GC-2014TF/SPL equipment, with splitless injection, a capillary column PETROCOL DH 50.2 and a FID detector.

3. Results and discussion

3.1. TGA

Figure 2a shows thermograms of LDPE together with those of its mixtures with some of the most representative solid materials which were studied, meanwhile, Figure 2b shows their mass loss velocity (DrTG) dependence with temperature. LDPE shows a weight loss starting above 400 °C due to the release of volatile products of the pyrolysis process. The temperature corresponding to the maximum rate of weight loss (T_M) is 486 °C. A similar profile is observed in the case of the LDPE-AC1 mixture although T_M is slightly lower, 473 °C, suggesting that some catalytic effect of the activated carbon on the rate of the LDPE pyrolysis might be taking place. In presence of the FCC and the Al-PILC catalysts, T_M drops to much lower values, 442 °C and 436 °C, respectively, with weight losses which are already appreciable at 310 °C and 325 °C, respectively, thus revealing a much higher catalytic effect of these solid materials than that of AC1. Table 1 shows T_M values for all the solid materials that were tested. As shown, the commercial activated carbon DARCO, AC2, AC3 did not lead to a significant decrease of T_M concerning that of LDPE alone. These results would exclude carbon-based materials here tested as suitable catalysts for LDPE pyrolysis. Something similar can be said for Fe-PILC and the calcium-rich montmorillonite (Mont). For the first one, the method here used for its preparation as well as the relative amount of iron can strongly affect its textural properties, mainly its acidic strength, which is one of the key parameters associated with its capacity to catalyze cracking reactions of hydrocarbons [28]. In this sense, a recent work reveals significant changes in textural properties of Fe-PILCs depending on their iron content [35].

3.2. N_2 adsorption-desorption isotherms

N_2 adsorption-desorption isotherms were performed for the most active materials according to results of TGA analysis, FCC and Al-PILC. They are shown in Figure 3 together with that of one of the activated carbons which were prepared, AC1. The isotherm of the commercial cracking catalyst (FCC) is of type I, typical of solids with a high proportion of micropores. It shows hysteresis of type H4, which is usually found in agglomerates having parallel platelets [39]. The isotherm of Al-PILC is similar to that of FCC with a high proportion of micropores although the hysteresis loop is almost indistinguishable. AC1 shows a III/IV type isotherm with strong adsorption at relative low pressure, which indicates a significant amount of micropore volume. A significant amount of N_2 is adsorbed in the range of medium pressures which indicates the presence of mesopores. Table 2 summarizes the textural parameters obtained from the isotherms: AC1 has the highest BET area (806 m^2 g^{-1}), followed by FCC and Al-PILC (245 and 179 m^2 g^{-1}, respectively). AC1 has also the highest micropore and total pore volume (0.33 and 1.09 cm^3 g^{-1}, respectively).

3.3. TPD-NH_3

TPD-NH_3 analyzes were performed for the 3 materials mentioned above. Figure 4 shows that all of them have a complex desorption profile indicating the presence of acid sites of different strength. FCC has the highest total amount of acid sites (713 μmol g^{-1}cat), followed by the Al-PILC (375 μmol g^{-1}cat) and the activated carbon with very low concentration (124 μmol g^{-1}cat). Deconvolution into Gaussian peaks was

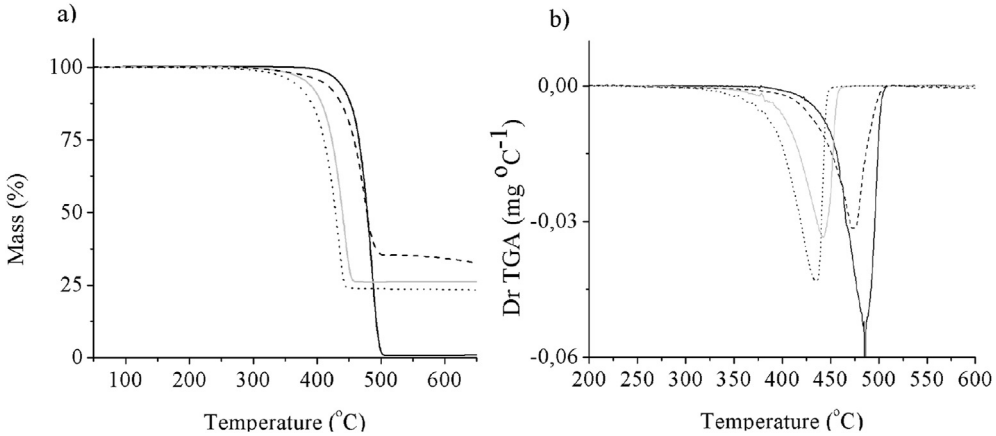

Figure 2. a) Thermogravimetric analysis and b) Derivative thermogravimetric analysis of LDPE alone and in the presence of 25 Wt% of different solids. In decreasing order of T_M: ▬ LDPE, - - LDPE-AC1, — LDPE-FCC, • • LDPE-Al-PILC.

Table 1. Weight loss maximum rate temperature (T_M) for LDPE alone and in the presence of 25 wt% of different solids.

Catalysts	–	FCC	DARCO	AC1	AC2	AC3	Mont	Al-PILC	Fe-PILC
T_M (°C^{-1})	486	442	486	473	486	485	471	436	476

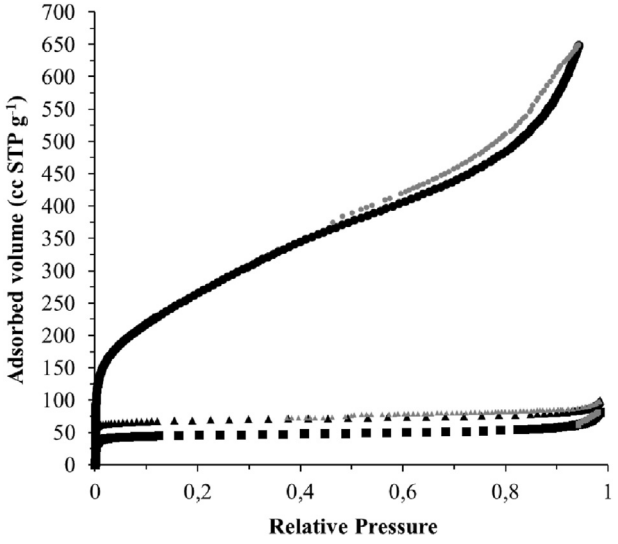

Figure 3. N_2 adsorption-desorption isotherms of FCC (▲), Al-PILC (■) and AC1 (●).

performed to allow a better acid site quantification in terms of their strength and relative amount, enabling deeper comparison between them (see Figure S1 to S3 in supplementary material). Table 3 summarizes the relative contribution of peaks resulting from deconvoluted profiles. FCC has a high proportion of strong sites (75%) corresponding to desorption maximum peak temperatures (T_D) higher than 398 °C. Al-PILC has a more distributed proportion of average and strong acid sites (25% for T_D in 251 °C and 70% for T_D higher than 355 °C). AC1 displays a maximum desorption peak corresponding to weak acid sites (T_D = 193 °C) while that at high temperature (T_D = 723 °C) should not be considered since it may be involved mainly with NH_3 released by chemical decomposition of the complex chemical structure of the carbon material at temperatures above the maximum reached in its preparation (450 °C). Strong acidity in the FCC catalyst is related with protons forming part of hydroxyl groups linked to framework aluminum atoms in zeolitic materials which are the main component of FCC catalysts [40, 41, 42]. Lewis acidity is also present, mainly after thermal treatment leading to dehydroxylation of the Brønsted sites. In the Al-PILC, Lewis acid sites are mainly resident on the Al oxide pillars, whereas Brønsted acid sites are associated with structural OH groups on the layers of the host clay [43]. Weak surface acidity in the activated carbon AC1 is mainly due to surface oxygen-containing functional groups such as carbonyl, carboxyl, phenolic hydroxyl, lactone and quinine groups [44, 45]. Fig. S4 (supplementary material) shows the IR spectra of these 3 materials. For Al-PILC and FCC, different bands at 3000-3600 cm^{-1} can be assigned to stretching vibrational frequencies of hydroxyl groups associated with Si (Si–OH), Al (Al–OH) and bridged hydroxyl groups (Si–O(H)–Al), all of them responsible for Brønsted acidity with variable strength according to their location in the solid structure [46, 47, 48]. For the activated carbon AC1, the spectrum shows a band at 1600-1580 cm^{-1} assigned to C–C vibrations in aromatic rings. The band at 1000-1300 cm^{-1} (maxima at 1190-1200 cm^{-1}) can be assigned to C–O stretching in acids, alcohols, phenols, ethers and/or esters groups [49]. The peak at 1190-1200 cm^{-1} may be also assigned to the stretching mode of hydrogen-bonded P=O, to O–C stretching vibrations in P–O–C (aromatic) linkage and to P=OOH. The shoulder at 1100 cm^{-1} was ascribed to ionized linkage P–O- in acid phosphate esters, and to symmetrical vibration in a P–O–P chain [50].

3.4. Pyrolysis tests

Based on the results of TGA materials sampling, a temperature of 430 °C was selected to carry out the pyrolysis tests with the most active materials (FCC and Al-PILC). Figure 5 shows the results obtained in the pyrolysis of LDPE alone. A gradual increase of the rate of liquid production is observed with a maximum of 0.184 cm^3 min^{-1}, after which it decreases due to the decrease in the amount of reactant plastic. No significant differences were observed in a pyrolysis test performed in presence of AC1 at the same reaction conditions, thus suggesting that its catalytic activity is not relevant and in agreement with TGA results. Figure 6 shows the results obtained with the commercial FCC catalyst. It can be observed that a much higher rate of liquid production is observed since the beginning of the test, already appreciable at 290 °C, and a maximum of 0.92 cm^3 min^{-1} which is much higher than that obtained with LDPE alone. The time needed to complete the test is also modified (62 min for FCC against 120 min without catalyst). An even more marked rate increment is observed with the Al-PILC (Figure 7), with a maximum rate (1.65 cm^3 min^{-1}) that almost doubles that obtained with the commercial FCC catalyst. The superior catalytic activity of the FCC and Al-PILC catalysts is consistent with the lower temperature of the

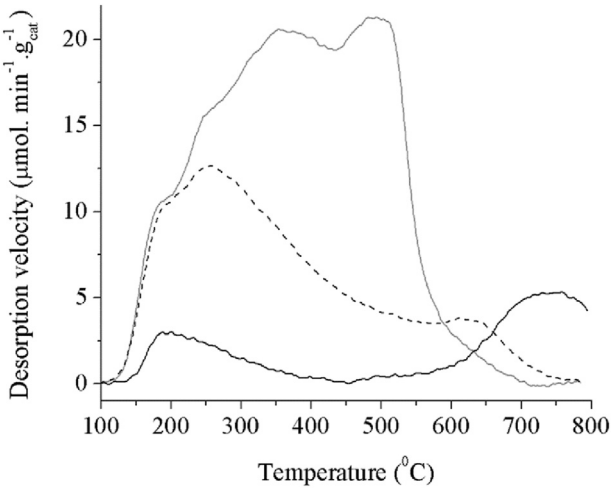

Figure 4. TPD-NH_3 profiles of catalysts: ——AC1, - - - Al-PILC and —— FCC.

Table 2. Textural physical properties of AC1, FCC and Al-PILC.

Material	BET area (m^2.g^{-1})	V_{DR} (cm^3.g^{-1})	V_T (cm^3.g^{-1})
AC1	806	0.33	1.09
FCC	245	0.11	0.16
Al-PILC	179	0.07	0.13

Table 3. TPD-NH_3 peak Gaussian deconvolution and total NH_3 desorption ($NH_{3,d}$).

Catalyst	NH_3 from deconvoluted peaks (μmol.g^{-1})								Total $NH_{3\ des}$ (μmol.g^{-1})	
	Peak 1		Peak 2		Peak 3		Peak 4			
	T_D	$NH_{3,d}$	T_D	$NH_{3,d}$	T_D	$NH_{3,d}$	T_D	$NH_{3,d}$	Meas.	Deconv.
FCC	186	20	251	81.6	398	548	516	76.3	713.2	726
Al-PILC	189	21.5	251	105	355	205	615	90.8	375.4	422.9
AC1	193	12.1	257	33.2	—	—	723	45.1	124.5	90.4

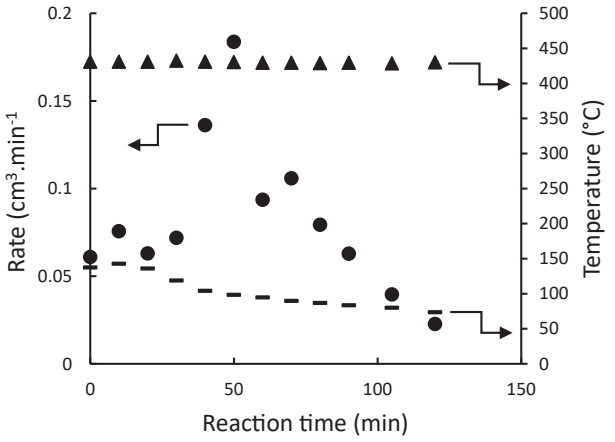

Figure 5. Pyrolysis test of LDPE (15 g) without catalyst. Experimental conditions: 430 °C and 300 Torr. (●) rate of liquid production; (▲) balloon temp.; (▬) elbow temp.

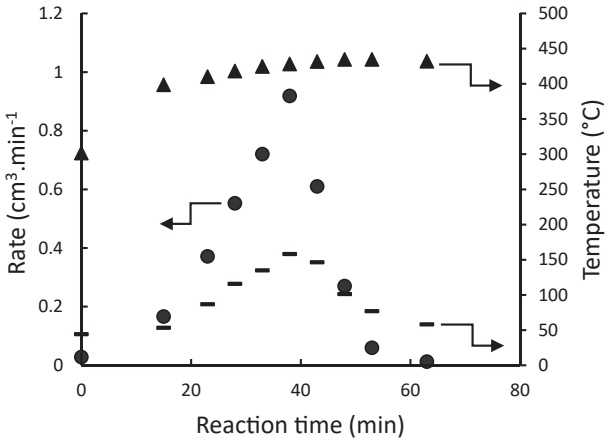

Figure 6. Pyrolysis test of a mixture of LDPE (15 g) and FCC (5 g). Experimental conditions: 430 °C and 300 Torr. (●) rate of liquid production; (▲) balloon temp.; (▬) elbow temp.

maximum weight loss rate (T_M), observed in TGA results and the higher amount of acid sites as observed by TPD-NH_3 analyzes.

Complementary pyrolysis tests were performed in the presence of the Al-PILC to assess the influence of the temperature on the process rate. Figure S5 (supplementary material) shows the results obtained at 400 °C, with a lower rate of liquid production (maximum of 0.65 cm^3 min^{-1}) and longer reaction time (92 min). At 370 °C (Figure S6 in supplementary material) the rate is noticeably smaller (maximum below 0.1 cm^3 min^{-1}) and unlike the previous tests the rate decreases from the beginning of the test. Probably, deactivation is taking place at this temperature by the formation of low volatile products that are not rapidly released from the catalyst surface and block active sites.

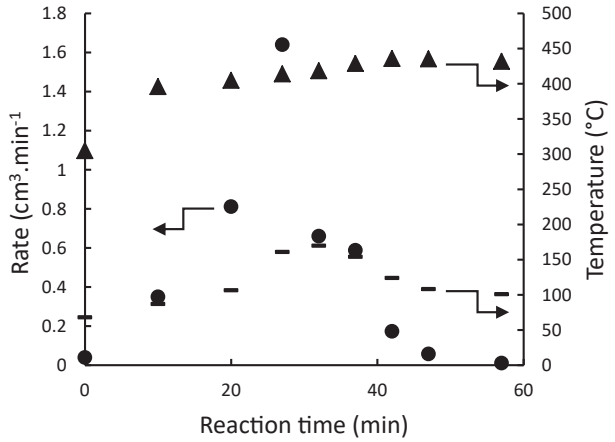

Figure 7. Pyrolysis test of a mixture of LDPE (15 g) and Al-PILC (5 g). Experimental conditions: 430 °C and 300 Torr. (●) rate of liquid production; (▲) balloon temp.; (▬) elbow temp.

Table 4 summarizes the weight yields of liquid products for the most relevant pyrolysis tests. In the absence of catalyst, 24% of liquid products were obtained while the residual mass in the reaction balloon was too small (1.5 %). The rest of the products corresponds to a significant amount (not precisely quantified) of a pale yellow solid embedded in the condenser that must contain high molecular weight hydrocarbons (C18+), and also light hydrocarbons that are not retained by condensation at the temperature of the receiving balloon (0 °C). A higher amount of liquid product was obtained in presence of the FCC (44.7 %), together with an unquantified amount of the pale-yellow solid in the condenser and light hydrocarbons. The highest yield of liquid products was obtained with the Al-PILC (70.2%), while the pale-yellow solid was reduced to a much lower amount, forming a thin layer coating the inner wall of the condenser. The yield of liquid products with the Al-PILC was still significant at 400 °C (61.9%) while a greater amount of solid was retained in the condenser. At 370 °C, the plastic was not completely converted into volatile products (37.1% of solid residue into the reaction balloon) and the yield of liquid product was even smaller (31%).

All these results reveal marked differences in the catalytic activity of the tested solids. Both, the rate of pyrolysis and product composition are greatly influenced by catalyst properties. The acidity of the catalyst plays a major role in its activity for the conversion of plastics, with higher catalyst acidity resulting in higher catalytic activity. Typically, catalytic cracking of polyolefins proceeds through a mechanism with initiation, disproportionation, β-scission, and termination reactions. Initiation involves the protolysis of the polymer macromolecule by hydrogen exchange with acid sites (Brønsted or Lewis) of the catalyst to yield paraffins and surface carbocations. Subsequently, carbocations undergo disproportionation or beta-scission reactions to yield smaller paraffins or olefins. All these primary products can undergo secondary reactions (such as dehydrogenation, oligomerization, isomerization, cyclization, aromatization) to yield the complex mixture of hydrocarbons that is finally obtained [51]. Acid sites strength is a key parameter affecting the

Table 4. Operation time, maximum volumetric production velocity and weight yields of liquid products for pyrolysis tests.

Material	Operation temperature (°C).	Operation time (h)	Maximum volumetric velocity (cm^3/min)	Liquid yield (%)
No solid	430	2.00	0.18	24.7
FCC	430	1.05	0.92	44.7
AL-PILC	430	0.62	1.64	70.2
AL-PILC	400	1.53	0.65	61.9
AL-PILC	370	4.02	0.09	31.0

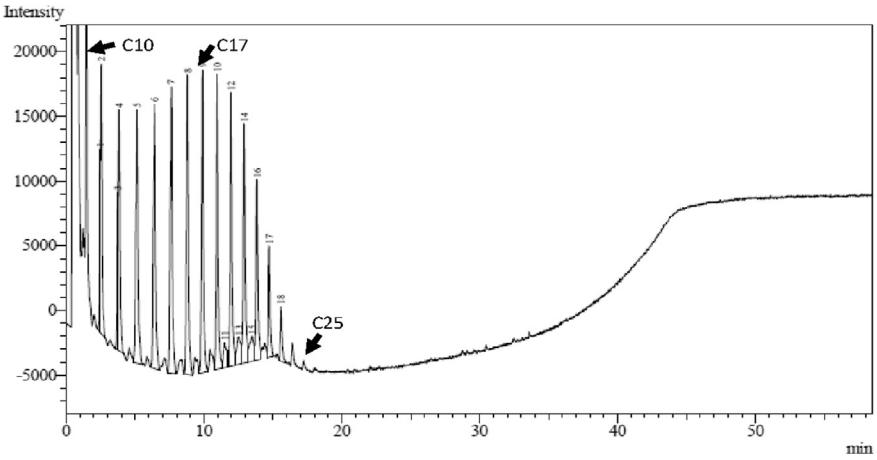

Figure 8. Typical chromatogram of liquid products of LDPE pyrolysis in the presence of an activated carbon at 430 °C and 300 torr.

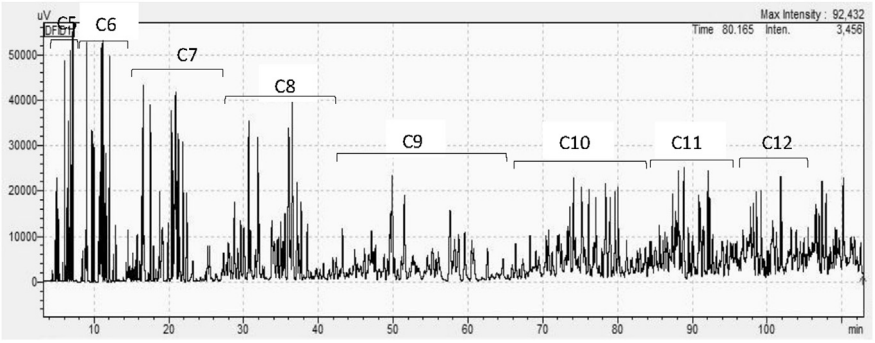

Figure 9. Typical chromatogram of liquid products of LDPE pyrolysis in the presence of an aluminum pillared clay at 430 °C and 300 torr.

rate of the different reactions and, thereby, the efficiency and selectivity of the global catalytic pyrolysis process. Another important property of catalysts is the micropore structure that affects the accessibility of hydrocarbons molecules to the active sites in the internal cavities [52, 53]. Regarding the activated carbon AC1, taking into account its high specific surface area and pore volume (see Table 1), the low catalytic activity must be ascribed to the lower amount and intrinsic activity of active sites involved in the pyrolysis reaction mechanism. As shown in Figure 4 and Table 3, this catalyst has the lowest total acidity, which, in addition, is given mainly by weak acid sites. Surface atoms associated with these weak acid sites would not have enough ability to interact with hydrocarbon molecules and form carbocations species that initiates the cracking reaction mechanism. In the case of the Al-PILC, acidity favors cracking reactions, leading to higher pyrolysis rates as well as a higher liquid hydrocarbons amount. Brønsted (B) and Lewis (L) acid sites are present in Al-PILCs, (L) sites proportion increase along with Al concentration in the dispersion used for pillared clays preparation. In the case of the FCC catalyst, its high content of strong acid sites can favor an over-cracking activity, leading to a higher proportion of light hydrocarbons which cannot be retained at the receiving balloon. Manos et al. also reported the higher yields of liquid product obtained with an Al-pillared clay compared with that obtained with a highly acidic zeolite [54]. Other comparative studies between Al-pillared clays and zeolites also showed a lower cracking activity of the pillared clay although both types of catalysts are equally active in more facile secondary reactions as a consequence of weakly acidic Lewis sites obviously present on pillared clays as well as on zeolites [55]. High acidity can also promote a higher extent of secondary reactions leading to the formation of carbon deposits on the catalyst surface with its consequent deactivation [56].

3.5. Liquid product characterization

Liquid products were characterized by their higher heating value. Values were all in the range of 42160–46047 kJ Kg^{-1}, which were similar to that of a commercial gasoil 44370 kJ Kg^{-1} (see Table S1 in supplementary material). The elemental analysis showed similar mass percent compositions: C: 84.2–84.5%; H: 15.4–15.7%; N: <0.10; S: —; corresponding to the H/C ratio (by weight) of 0.18–0.19, also close to that of the commercial gasoil (0.17). Chromatographic analysis performed in the experimental conditions (i) showed significant differences among the different catalysts. In the absence of catalysts and with the carbon material AC1, a well-defined series of peaks, each one corresponding to a

hydrocarbon with a different number of carbon atoms (n), was observed; n values were between 5 and 28 (Figure 8). The literature reports similar results corresponding to a broad distribution of aliphatic hydrocarbons within a wide C_n range (n: 5 to 80), each fraction being formed by the corresponding n-paraffin, diene and 1-olefin [57, 58, 59]. A radical chain reaction mechanism comprising hydrogen transfer steps along with the progressive breaking of the polymer backbone explains these experimental results satisfactorily [60]. Products distribution profiles close to that shown in Figure 8 are also reported using a series of solids materials having weak surface acidity (silica gel, 5A molecular sieve and activated carbon) [61]. In this case, weak acid sites would be active mainly to catalyze secondary reactions of cracking products. Analyzes performed in the experimental conditions (ii) allowed to observe that liquid products obtained with the FCC and the Al-PILC display a high amount of peaks for each number of carbon atoms in the range C5–C13, thus revealing the presence of a more complex mixture of compounds formed by secondary reactions of the primary hydrocarbon fragments (Figure 9). In the presence of several zeolite catalysts, a marked increase in the aromatic content of the derived oils is reported together with a decrease of aliphatic compounds concentration and a shift in carbon numbers from high to low values [38, 62, 63]. FCC catalysts containing zeolitic materials as the main active component follow the same trend regarding the amount of products in the gaseous and liquid evolution although the more equilibrated acid site structure compared with the zeolite allows to minimize coke deposition and increase the resistance to deactivation and regenerability [64].

The presence of functional groups in the produced liquid oils from catalytic pyrolysis was characterized using FTIR analysis. Figure S7 (supplementary material) shows that spectra are dominated by signals corresponding to C–H stretching (3000-2800 cm^{-1}) and C–H bending (1465 cm^{-1}, 1375 cm^{-1}). Differences are found in signals in the range from 900 to 1000 cm^{-1}. For the liquid products obtained without catalyst and with the activated carbon it can be observed a signal at 910 cm^{-1} corresponding to terminal olefins ($R–CH = CH_2$). This signal does not appear in products obtained with Al-PILC and FCC catalysts and suggests that the concentration of linear olefins was drastically decreased. Several other products could be formed as a result of secondary reactions catalyzed by average and strong acid sites of these two catalysts thus leading to the more complex mixture of products shown in Figure 9.

4. Conclusions

The catalytic degradation of LDPE was studied in the presence of several solid materials. Thermogravimetric analysis showed that an aluminum-pillared clay (Al-PILC) and a commercial cracking catalyst (FCC) have a marked catalytic effect leading to a significant reduction of the degradation temperature compared with some activated carbons and other clay based materials. The highest amount of surface acid sites in the Al-PILC and FCC materials explains these catalytic effect. Pyrolysis tests confirmed the higher catalytic activity of the Al-PILC and FCC and allowed the obtention of significant amounts of liquid products. The aluminum-pillared clay, having the highest proportion of intermediate acid strength sites, led to a liquid hydrocarbon recovery of 70 wt.% at 430 °C and 300 torr, which was the highest liquid yield obtained. Aliphatic hydrocarbons ranging from C5 to C28 were identified in the liquid products from the pyrolysis in presence of an activated carbon, while a more complex composition was obtained in the presence of FCC and Al-PILC.

Declarations

Author Contribution statement

Melisa Olivera: Performed the experiments; Analyzed and interpreted the data; Wrote the paper.

Mauricio Musso: Performed the experiments.

Andrea De León: Contributed reagents, materials, analysis tools or data.

Alejandro Amaya & Elisa Volonterio: Performed the experiments; Analyzed and interpreted the data.

Nestor Tancredi: Contributed reagents, materials, analysis tools or data; Wrote the paper.

Juan Bussi: Conceived and designed the experiments; Analyzed and interpreted the data; Wrote the paper.

Funding statement

This work was supported by the Comisión Sectorial de Investigación Científica (Project I+D 1512), Universidad de la República, Uruguay.

Competing interest statement

The authors declare no conflict of interest.

Additional information

Supplementary content related to this article has been published online at https://doi.org/10.1016/j.heliyon.2020.e05080.

Acknowledgements

The authors thank Dr. Carlos Apesteguía, Director of the GICIC Research Group, INCAPE (UNL-CONICET), Santiago del Estero 2654, Santa Fe, Argentina, for TPD-NH_3 characterization of catalysts.

References

[1] Sh.D.A. Sharuddin, F. Abnisa, W.M.A.W. Daud, M.K. Aroua, A review on pyrolysis of plastic wastes, Energy Convers. Manag. 115 (2016) 308–326.
[2] A. López, I. de Marco, B. Caballero, M. Laresgoiti, A. Adrados, Influence of time and temperature on pyrolysis of plastic wastes in a semi-batch reactor, Chem. Eng. J. 173 (2011) 62–71.
[3] W. Kaminsky, B. Schlesselmann, C. Simon, Olefins from polyolefins and mixedplastics by pyrolysis, J. Anal. Appl. Pyrol. 32 (1995) 19–27.
[4] S. Kumar, R.K. Singh, Recovery of hydrocarbon liquid from waste high density polyethylene by thermal pyrolysis, Braz. J. Chem. Eng. 28 (4) (2011) 659–667.
[5] I. Kalargaris, G. Tian, S. Gu, The utilisation of oils produced from plastic waste at different pyrolysis temperatures in a DI diesel engine, Energy 131 (2017) 179–185.
[6] A.K. Panda, R.K. Singh, D.K. Mishra, Thermolysis of waste plastics to liquid fuel. A suitable method for plastic waste management and manufacture of value added products—a world prospective, Renew. Sustain. Energy Rev. 14 (2010) 233–248.
[7] U. Arena, M.L. Mastellone, Fluidized bed pyrolysis of plastic wastes, in: J. Scheirs (Ed.), Feedstock Recycling and Pyrolysis of Waste Plastics: Converting Waste Plastics into Diesel and Other Fuels, John Wiley & Sons, Ltd, Canada, 2006, pp. 435–471.
[8] R. Thahir, A. Altway, S.R. Juliastuti, D. Susianto, Production of liquid fuel from plastic waste using integrated pyrolysis method with refinery distillation bubble cap plate column, Energy Rep. 5 (2019) 70–77.
[9] M.A. Hazrat, M.G. Rasul, M.M.K. Khan, A study on thermo-catalytic degradation for production of clean transport fuel and reducing plastic wastes, Procedia Eng. 105 (2015) 865–876.
[10] B. Kunwar, B.R. Moser, S.R. Chandrasekaran, N. Rajagopalan, B.K. Sharma, Catalytic and thermal depolymerization of low value post-consumer high density polyethylene plastic, Energy 111 (2016) 884–892.
[11] R. Miandad, M.A. Barakat, A.S. Aburiazaiza, M. Rehan, A.S. Nizami, Catalytic pyrolysis of plastic waste: a review, Process Saf. Environ. 102 (2016) 822–838.
[12] S.M. Al-Salem, A. Antelava, A. Constantinou, G. Manos, A. Dutta, A review on thermal and catalytic pyrolysis of plastic solid waste (PSW), J. Environ. Manag. 197 (2017) 177–198.
[13] A.S. Burange, M.B. Gawande, F.L.Y. Lam, R.V. Jayaram, R. Luque, Heterogeneously catalyzed strategies for the deconstruction of high density polyethylene: plastic waste valorisation to fuels, Green Chem. 17 (2015) 146–156.
[14] P.S. Kumar, M. Bharathikumar, C. Prabhakaran, S. Vijayan, K. Ramakrishnan, Conversion of waste plastics into low-emissive hydrocarbon fuels through catalytic depolymerization in a new laboratory scale batch reactor, Int. J. Energy Environ. Eng. 8 (2017) 167–173.
[15] D.K. Ratnasari, M.A. Nahil, P.T. Williams, Catalytic pyrolysis of waste plastics using staged catalysis for production of gasoline range hydrocarbon oils, J. Anal. Appl. Pyrolysis 124 (2017) 631–637.
[16] R. Miandad, M.A. Barakat, M. Rehan, A.S. Aburiazaiza, I.M.I. Ismail, A.S. Nizami, Plastic waste to liquid oil through catalytic pyrolysis using natural and synthetic zeolite catalysts, Waste Manag. 69 (2017) 66–78.

[17] G. Manos, A. Garforth, J. Dwyer, Catalytic degradation of high-density polyethylene over different zeolitic structures, Ind. Eng. Chem. Res. 39 (2000) 1198–1202.
[18] G. Manos, A. Garforth, J. Dwyer, Catalytic degradation of high-density polyethylene on an ultrastable-Y zeolite. Nature of initial polymer reactions, pattern of formation of gas and liquid products, and temperature effects, Ind. Eng. Chem. Res. 39 (2000) 1203–1208.
[19] A. López, I. de Marco, B.M. Caballero, M.F. Laresgoiti, A. Adradoa, A. Aranzabal, Catalytic pyrolysis of plastic wastes with two different types of catalysts: ZSM-5 zeolite and Red Mud, Appl. Catal. B Environ. 104 (2011) 211–219.
[20] G. Elordi, M. Olazar, M. Artetxe, P. Castaño, J. Bilbao, Effect of the acidity of the HZSM-5 zeolite catalyst on the cracking of high density polyethylene in a conical spouted bed reactor, App. Catal. A-Gen. 415 – 416 (2012) 89–95.
[21] D. Almeida, M.F. Marques, Thermal and catalytic pyrolysis of plastic waste, Polímeros 26 (1) (2016) 44–51.
[22] Ch. Santella, L. Cafiero, D. De Angelis, F. La Marca, R. Tuffi, S.V. Ciprioti, Thermal and catalytic pyrolysis of a mixture of plastics from small waste electrical and electronic equipment (WEEE), Waste Manag. 54 (2016) 143–152.
[23] A.K. Panda, A. Alotaibi, I. V Kozhevnikov, N. Raveendran Shiju, Pyrolysis of plastics to liquid fuel using sulphated zirconium hydroxide catalyst, Waste Biomass Valor (2019).
[24] M. Sarker, M.M. Rashid, Waste plastics mixture of polystyrene and polypropylene into light grade fuel using Fe2O3 catalyst, Int. J. Renew. Energy Technol. Res. 2 (1) (2013) 17–28 (Online).
[25] Y. Sander González, C. Costa, M. Carmen Márquez, P. Ramos, Thermal and catalytic degradation of polyethylene wastes in the presence of silica gel, 5A molecular sieve and activated carbon, J. Hazard Mater. 187 (2011) 101–112.
[26] G. Manos, I.Y. Yusof, N. Papayannakos, N.H. Gangas, Catalytic cracking of polyethylene over clay catalysts. Comparison with an ultrastable Y zeolite, Ind. Eng. Chem. Res. 40 (2001) 2220–2225.
[27] G. Manos, I.Y. Yusof, N.H. Gangas, N. Papayannakos, Tertiary recycling of polyethylene to hydrocarbon fuel by catalytic cracking over aluminum pillared clays, Energy Fuel. 16 (2002) 485–489.
[28] K. Li, J. Lei, G. Yuan, P. Weerachanchai, J.-Y. Wang, J. Zhao, Y. Yang, Fe-, Ti-, Zr- and Al-pillared clays for efficient catalytic pyrolysis of mixed plastics, Chem. Eng. J. 317 (2017) 800–809.
[29] A.K. Panda, Thermo-catalytic degradation of different plastics to drop in liquid fuel using calcium bentonite catalyst, Int. J. Ind. Chem. 9 (2) (2018) 167–176.
[30] S. Budsaereechai, A.J. Hunt, Y. Ngernyen, Catalytic pyrolysis of plastic waste for the production of liquid fuels for engines, RSC Adv. 9 (2019) 5844–5857.
[31] H. Marsh, F. Rodriguez-Reinoso, Activated Carbon, Elsevier Science & Technology Books, 2006.
[32] S.A. Dastgheib, D.A. Rockstraw, Pecan shell activated carbon: synthesis, characterization, and application for the removal of copper from aqueous solution, Carbon 39 (2001) 1849–1855.
[33] M.A. De León, C. De Los Santos, L. Latrónica, A.M. Cesio, C. Volzone, J. Castiglioni, M. Sergio, High catalytic activity at low temperature in oxidative dehydrogenation of propane with Cr-Al pillared clay, Chem. Eng. J. 241 (2014) 336–343.
[34] M.A. De León, M. Sergio, J. Bussi, G.B. Ortiz de la Plata, A.E. Cassano, O.M. Alfano, Application of a montmorillonite clay modified with iron in photo-Fenton process, Comparison with goethite and nZVI, Environ. Sci. Pollut. Res. 22 (2015) 864–869.
[35] M.A. De León, M. Rodríguez, S.G. Marchetti, K. Sapag, R. Faccio, M. Sergio, J. Bussi, Raw montmorillonite modified with iron for photo-Fenton processes: influence of iron content on textural, structural and catalytic properties, J. Environ. Chem. Eng. 5 (2017) 4742–4750.
[36] K. Murata, K. Sato, Y. Sakata, Effect of pressure on thermal degradation of polyethylene, J. Anal. Appl. Pyrol. 71 (2004) 569–589.
[37] N.S. Akpanudoh, K. Gobin, G. Manos, Catalytic degradation of plastic waste to liquid fuel over commercial cracking catalysts. Effect of polymer to catalyst ratio/ acidity content, J. Mol. Catal. A Chem. 235 (2005) 67–73.
[38] G. Manos, Catalytic degradation of plastic waste to fuel over microporous materials, in: J. Scheirs, W. Kaminsky (Eds.), Feedstock Recycling and Pyrolysis of Waste Plastics: Converting Waste Plastics into Diesel and Other Fuels, Wiley, 2006, pp. 193–206.
[39] S.J. Gregg, K.S.W. Sing, Adsorption Surface Area and Porosity, Academic Press, London, U.K., 1982.
[40] E.G. Derouane, J.C. Védrine, R. Ramos Pinto, P.M. Borges, L. Costa, M.A.N.D.A. Lemos, F. Lemos, F. Ramôa Ribeiro, The acidity of zeolites: concepts, measurements and relation to catalysis: a review on experimental and theoretical methods for the study of zeolite acidity, Catal. Rev. Sci. Eng. 55 (4) (2013) 454–515.
[41] E.F. Sousa-Aguiar, Y Zeolites as a major component of FCC catalysts: main challenges in the modification thereof, in: B.F. Sels, L.M. Kustov (Eds.), Zeolites and Zeolite-like Materials, Elsevier, 2016, pp. 265–282.
[42] E.T.C. Vogt, B.M. Weckhuysen, Fluid catalytic cracking: recent developments on the grand old lady of zeolite catalysis, Chem. Soc. Rev. 44 (2015) 7342–7370.
[43] H. Ming-Yuan, L. Zhonghui, M. Enzen, Acidic and hydrocarbon catalytic properties of pillared clay, Catal. Today 2 (1988) 321–338.
[44] Ch.-Ch. Huang, H.-S. Li, Ch.-H. Chen, Effect of surface acidic oxides of activated carbon on adsorption of ammonia, J. Hazard Mater. 159 (2008) 523–527.
[45] Y.V. Kissin, Chemical mechanisms of catalytic cracking over solid acidic catalysts: alkanes and alkenes, Catal. Rev. 43 (1-2) (2001) 85–146.
[46] J.-F. Lambert, G. Poncelet, Acidity in pillared clays: origin and catalytic manifestations, Top. Catal. 4 (1997) 43–56.
[47] M. Boronat, A. Corma, Factors controlling the acidity of zeolites, Catal. Lett. 145 (2015) 162–172.
[48] E.G. Derouane, J.C. Védrine, R. Ramos Pinto, P.M. Borges, L. Costa, M.A.N.D.A. Lemos, F. Lemos, F. Ramôa Ribeiro, The acidity of zeolites: concepts, measurements and relation to catalysis: a review on experimental and theoretical methods for the study of zeolite acidity, Catal. Rev. 55 (4) (2013) 454–515.
[49] S.M. Yakout, G. Sharaf El-Deen, Characterization of activated carbon prepared by phosphoric acid activation of olive stones, Arab. J. Chem. 9 (2016) S1155–S1162.
[50] S. Bourbigot, M.L. Bras, R. Delobel, Carbonization mechanisms resulting from intumescence. II. Association with an ethylene terpolymer and the ammonium polyphosphate-pentaerythritol fire retardant system, Carbon 33 (3) (1995) 283–294.
[51] J. Walendziewski, Thermal and catalytic conversion of polyolefins, in: J. Scheirs, W. Kaminsky (Eds.), Feedstock Recycling and Pyrolysis of Waste Plastics: Converting Waste Plastics into Diesel and Other Fuels, Wiley, 2006, pp. 111–271.
[52] K. Pyra, K.A. Tarach, D. Majda, K. Góra-Marek, Desilicated zeolite BEA for the catalytic cracking of LDPE: the interplay between acidic sites' strength and accessibility, Catal. Sci. Technol. 9 (2019) 1794–1801.
[53] D.P. Serrano, J. Aguado, J.M. Escola, Developing advanced catalysts for the conversion of polyolefinic waste plastics into fuels and chemicals, ACS Catal. 2 (2012) 1924–1941.
[54] G. Manos, I.Y. Yusof, N. Papayannakos, N.H. Gangas, Catalytic cracking of polyethylene over clay catalysts. Comparison with an ultrastable Y zeolite, Ind. Eng. Chem. Res. 40 (2001) 2220–2225.
[55] U. Kürschner, V. Seefeld, B. Parlitz, W. Geflner, H. Lieske, Catalytic activity and acidity of Al pillared clays and zeolites in different hydrocarbon reactions, React. Kinet. Catal. Lett. 65 (1) (1998) 17–23.
[56] A. López, I. de Marco, B.M. Caballero, A. Adrados, M.F. Laresgoiti, Deactivation and regeneration of ZSM-5 zeolite in catalytic pyrolysis of plastic wastes, Waste Manag. 31 (2011) 1852–1858.
[57] J. Aguado, D.P. Serrano, J.M. Escola, Catalytic upgrading of plastic wastes, in: J. Scheirs, W. Kaminsky, Orgs (Eds.), Feedstock Recycling and Pyrolysis of Waste Plastics: Converting Waste Plastics into Diesel and Other Fuels, John Wiley & Sons, 2006, pp. 73–110.
[58] N. Miskolczi, R. Nagy, Hydrocarbons obtained by waste plastic pyrolysis: comparative analysis of decomposition described by different kinetic models, Fuel Process. Technol. 104 (2012) 96–104.
[59] B.K. Sharma, B.R. Moser, K.E. Vermillion, K.M. Doll, N. Rajagopalan, Production, characterization and fuel properties of alternative diesel fuel from pyrolysis of waste plastic grocery bags, Fuel Process. Technol. 122 (2014) 79–90.
[60] T.P. Wampler, Thermometric behavior of polyolefins, J. Anal. Appl. Pyrol. 15 (1989) 187–195.
[61] Y. Sander González, C. Costa, M.C. Márquez, P. Ramos, Thermal and catalytic degradation of polyethylene wastes in the presence of silica gel, 5A molecular sieve and activated carbon, J. Hazard Mater. 187 (2011) 101–112.
[62] D.K. Ratnasari, M.A. Nahil, P.T. Williams, Catalytic pyrolysis of waste plastics using staged catalysis for production of gasoline range hydrocarbon oils, J. Anal. Appl. Pyrol. 124 (2017) 631–637.
[63] R. Bagri, P.T. Williams, Catalytic pyrolysis of polyethylene, J. Anal. Appl. Pyrol. 63 (2002) 29–41.
[64] G. Elordi, M. Olazar, P. Castaño, M. Artetxe, J. Bilbao, Polyethylene cracking on a spent FCC catalyst in a conical spouted bed, Ind. Eng. Chem. Res. 51 (2012) 14008–14017.